A COLD GAS THRUSTER MICROSATELLITE ATTITUDE CONTROL

ABDELLATIF BELLAR [1,2], MOHAMMED KARIM FELLAH [1],
MOHAMMED AREZKI SI MOHAMMED [2]

Key words: Microsatellite, Attitude control, Fuzzy pulse width pulse frequency (FPWPF), minimum time control.

This paper investigates the potential of fuzzy pulse width pulse frequency controller (FPWPFC) for a 3-axis thruster attitude control on low earth orbit satellites. The control objective is to point the satellite to the desired state within a minimum of time and with a minimum fuel consumption. A comparative study of the FPWPFC, the proportional derivative pulse width pulse frequency controller (PDPWPFC) and the proportional derivative bang-bang controller (PDBBC) with dead zone controller is performed to evaluate the performance of the attitude control system during a 3-axis attitude control. The robustness of FPWPFC has been validated using the Monte–Carlo method. Simulation results demonstrated the effectiveness and advantages of the proposed controller to minimize the fuel consumption.

1. **INTRODUCTION**

Attitude control is the process of orienting the spacecraft in a specified and predetermined direction. Reaction wheels are a common choice for active spacecraft attitude control [1, 2]. The reaction wheel has its own advantages and disadvantages. It is faster compared to the torque rods but slower compared to thrusters. A major advantage of the reaction wheel is that it is a linear actuating device unlike thrusters. The significant disadvantage of a reaction wheel is that it suffers mechanical wear-out when operated continuously over years. Another disadvantage is that it can generate only torques and not forces. An effective and rapid momentum dumping can be achieved by thrusters at the cost of expendable propellant consumption [3]. For satellites with thrusters, the minimization of propellant dissipation is critically important to the space mission. For a simple single-axis satellite problem, there is the unique minimum-time solution [4]. However, there is no obvious solution for a full three-axis problem. The two major approaches for thruster control are bang-bang control and pulse modulation. Bang-

[1] Djillalil Liabès University of Sidi Bel-Abbès, Algeria; E-mail: a_bellar@yahoo.fr
[2] Centre of Space Techniques, Arzew, Oran, Algeria

bang control [5, 6] is simple in formulation but the pulse modulators [7, 8] are commonly employed due to their advantages of reduced propellant consumption and near-linear duty cycle. On the other hand, pulsing technique used is a pulse width pulse frequency (PWPF) method, relevant literature claims that the PWPF modulator holds advantages over other types of pulse modulators [9–11], and it has also been demonstrated that it holds considerable advantages over bang-bang control systems. The idea behind using a dead-zone is to avoid unnecessary pulsing of the thrusters due to sensor noise. Also a time constant network is used prior to the hysteresis block to control the thruster firing frequency. Other works use the fuzzy controllers [12–15] witch are flexible, simple to build and provide robustness to the bang-bang controller. Artificial intelligence technique such as fuzzy logic has provided the means to develop flexible fuzzy bang-bang control (FBBC) [12, 15]. As a result, FBBC is usually applied to a complex system whose dynamic model is not well defined or not available at all [13, 14]. They have shown that the fuzzy controller tracked the reference command better than the conventional bang-bang controller, but with the use of higher thruster on/off cycles. In addition to handling nonlinear problems, the fuzzy control has proven its effectiveness and robustness of system [1, 16, 17]. However, the fuzzy logic control (FLC) rules and memberships which are the heart of the controller are usually generated from a skilful operator, engineering experience or by adaptation algorithms.

Our contribution in this paper it combines the advantages of both techniques, we design the fuzzy logic controller (FLC) plus pulse width pulse frequency modulator for a 3-axis thruster attitude control on low earth orbit satellite. We evaluate the performance of the control system during agile control and we used the quaternion error. In order to test the effectiveness of these controllers, its robustness in the presence of disturbances and fuel consumption, the system is subjected to an additional pseudorandom noise level of 2% and we used the Monte–Carlo method to compare the fuel consumption.

The remainder of the paper is organized as follows. Section 2 presents the attitude description and convention used in this paper, the dynamic and kinematic models used for the satellite will be given. The structure and design of proportional derivative bang-bang controller (PDBBC) and the proposed controller is presented and discussed in Section 3. Following these descriptions the simulation results are presented in Section 4. Finally, the conclusion of this work is presented in Section 5.

2. SATELLITE ATTITUDE DYNAMICS

In common with boats and aircraft the orientation of a spacecraft can be defined by three angles (roll, pitch, and yaw). These angles are obtained from a sequence of right hand positive rotations from a reference $\boldsymbol{X}_R$, $\boldsymbol{Y}_R$, $\boldsymbol{Z}_R$ frame to a

$\boldsymbol{X}_B$, $\boldsymbol{Y}_B$, $\boldsymbol{Z}_B$ set of spacecraft body axes. There are 12 possible sequences of rotations, which can be expressed using Euler angles. One example is a 2-1-3 sequence rotation. The first rotation is a pitch about the reference $\boldsymbol{Y}_R$ axis, this defines a pitch angle θ. The second rotation is a roll about the intermediate $\boldsymbol{L}$ axis, this define a roll angle φ. The last rotation is a yaw about the body $\boldsymbol{Z}_B$ axis, this define a yaw angle ψ. The attitude matrix, $\boldsymbol{A}$, which transforms an arbitrary vector from the reference $\boldsymbol{X}_R$, $\boldsymbol{Y}_R$, $\boldsymbol{Z}_R$ coordinates to the spacecraft body $\boldsymbol{X}_B$, $\boldsymbol{Y}_B$, $\boldsymbol{Z}_B$ coordinates can be expressed in term of Euler symmetric parameters as [18],

$$\boldsymbol{A} = \begin{bmatrix} c\psi c\theta + s\psi s\varphi s\theta & s\psi c\varphi & -c\psi s\theta + c\psi s\varphi c\theta \\ -s\psi c\theta + c\psi s\varphi s\theta & c\psi c\varphi & s\psi s\theta + c\psi s\varphi c\theta \\ c\varphi s\theta & -s\varphi & c\varphi c\theta \end{bmatrix}, \tag{1}$$

where c = cosine function; s = sine function.

The dynamics of the spacecraft in inertial space governed by Euler's equations of motion can be expressed as follows in vector form [18]

$$\boldsymbol{I}\dot{\omega}_{BI} = \boldsymbol{N}_{GG} + \boldsymbol{N}_{\mathrm{D}} + \boldsymbol{N}_M + \boldsymbol{N}_T - \omega_{BI} \times \left(\boldsymbol{I}\omega_{BI} + \boldsymbol{h}\right) - \dot{\boldsymbol{h}}, \tag{2}$$

where $\boldsymbol{\omega}_{BI}$ is the satellite body angular velocity vector, $\boldsymbol{I}$ is the inertia matrix, $\boldsymbol{N}_{GG}$ is the gravity gradient torque vector, $\boldsymbol{N}_D$ is the external disturbance torques vector, $\boldsymbol{N}_M$ is the torque vector by 3-axis magnetorquers, $\boldsymbol{h}$ is the wheel angular momentum and $\boldsymbol{N}_T$ applied torque vector by 3-axis thrusters.

The rate of change of the quaternion is given [18] as,

$$\dot{\mathbf{q}} = \frac{1}{2}\ \Lambda\,(q)\ \omega_{BO}, \tag{3}$$

$$\Lambda(q) = \begin{bmatrix} q_4 & -q_3 & q_2 \\ q_3 & q_4 & -q_1 \\ -q_2 & q_1 & q_4 \\ -q_1 & -q_2 & -q_3 \end{bmatrix}, \tag{4}$$

where $\boldsymbol{\omega}_{BI} = [\omega_{ox} \quad \omega_{oy} \quad \omega_{oz}]^{\mathrm{T}}$: body angular velocity vector referenced to orbital coordinates.

The angular body rates referenced to the orbit coordinates can be obtained from the inertially referenced body rates by using the transformation matrix $\boldsymbol{A}$ [18] is expressed as,

$$\omega_{BO} = \omega_{BI} - \boldsymbol{A}\,\omega_0, \tag{5}$$

where $\boldsymbol{\omega}_0 = [0 \quad \omega_0 \quad 0]^{\mathrm{T}}$ is an orbital rate vector.

When quaternion are used directly in the control algorithm it will be convenient to define an error quaternion. The error quaternion is calculated by using the definition of quaternion division [7] as,

$$\begin{bmatrix} q_{1e} \\ q_{2e} \\ q_{3e} \\ q_{4e} \end{bmatrix} = \begin{bmatrix} q_{4c} & q_{3c} & -q_{2c} & -q_{1c} \\ -q_{3c} & q_{4c} & q_{1c} & -q_{2c} \\ q_{2c} & -q_{1c} & q_{4c} & -q_{3c} \\ q_{1c} & q_{2c} & q_{3c} & q_{4c} \end{bmatrix} \begin{bmatrix} q_1 \\ q_2 \\ q_3 \\ q_4 \end{bmatrix}, \tag{6}$$

where: $\boldsymbol{q}_{ie}$= components of the error quaternion; $\boldsymbol{q}_{ic}$ = components of the commanded quaternion.

3. **CONTROLLER DESIGN**

3.1. PD BANG-BANG CONTROLLER

The thruster torque when using a single thruster was assumed to be constant value of 35 milli-Nm. The quaternion and angular velocity were used to compute the attitude errors in the law. A PDBBC was implemented with an attitude deadband of $\pm 1°$ in all axes. The non-linear control law can be summarized by the following set of equations [7] as,

$$\boldsymbol{e} = \boldsymbol{k}_d \boldsymbol{\omega}_{BO} + \boldsymbol{k}_p \boldsymbol{q}_e \,. \tag{7}$$

Then the thruster mode to apply a torque around the 3-axis is expressed as,

$$\mathbf{U} = \begin{cases} +1 & \text{for} \quad \mathbf{e} \geq 1.0 \\ 0 & \text{for} \quad -1.0 < \mathbf{e} < 1.0 \\ -1 & \text{for} \quad \mathbf{e} \leq -1.0 \,. \end{cases} \tag{8}$$

3.2. DESIGN OF FUZZY PULSE WIDTH PULSE FREQUENCY CONTROLLER (FPWPFC)

A fuzzy logic attitude controller has been developed where seven fuzzy labels: Negative Big (NB), Negative Medium (NM), Negative Small (NS), Zero (ZO). Positive Small (PS), Positive Mmall (PM) and Positive Big (PB) have been defined for the input-output variables. The FLC system has two inputs, quaternion error $\boldsymbol{q}_e(k)$ and angular velocity $\boldsymbol{\omega}_{BO}$ (k) and one output, $\boldsymbol{U}_c(k)$, as shown in Fig. 1. Also, 21 control rules were used which are shown in Table 1.

Table 1

Fuzzy contol rulles

$\omega_{BO}(k)$ \ $q_e(k)$	NB	NM	NS	ZO	PS	PM	PB
NB	NB	NB	NB	ZO	PS	PM	PB
ZO	NB	NM	NS	ZO	PS	PM	PB
PB	NB	NM	NS	ZO	PB	PB	PB

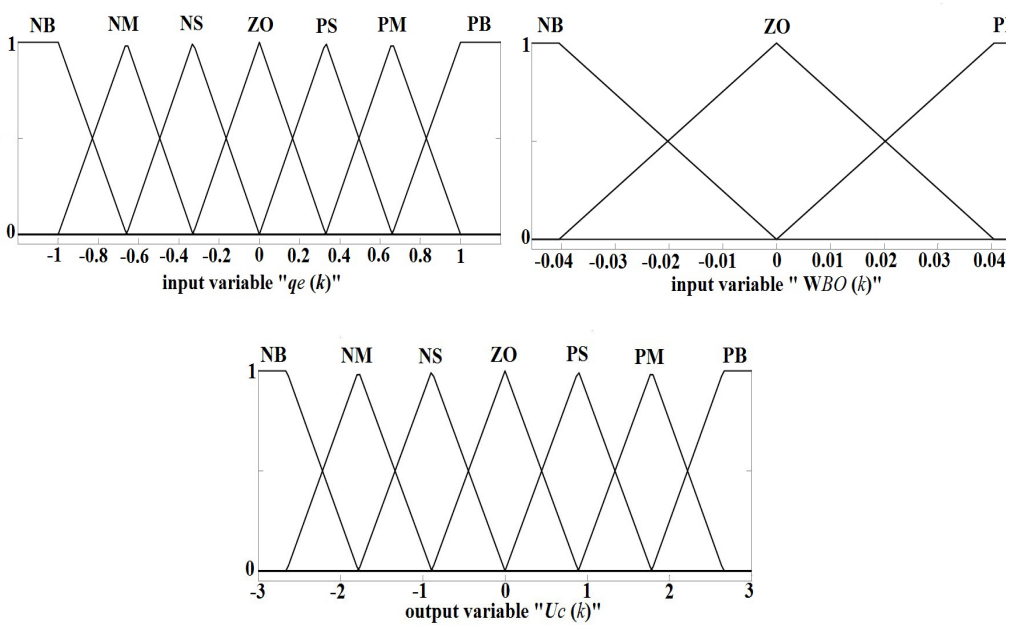

Fig 1 – Membership functions used in FLC.

The actuators are pulse cold gas (CG) thrusters and the pulsing of thrusters is done by a Schmidt trigger which has a dead-zone incorporated in it. The idea behind using a dead-zone is to avoid unnecessary pulsing of the thrusters due to sensor noise. Also a time constant network is used prior to the hysteresis block to control the thruster firing frequency. The most important task in this analysis is to relate the error in attitude to the on and off pulse periods. Figure 2 shows the FPWPFC block diagram.

A torque is generated only when the Schmitt trigger is activated. Once the trigger is activated a positive or negative pulse is generated thereby producing a torque. For periods when the trigger is not pulsed the satellite will drift as if it was in an open loop. We have also included a gain ***Knom***, which is simply the nominal thruster torques for a satellite.

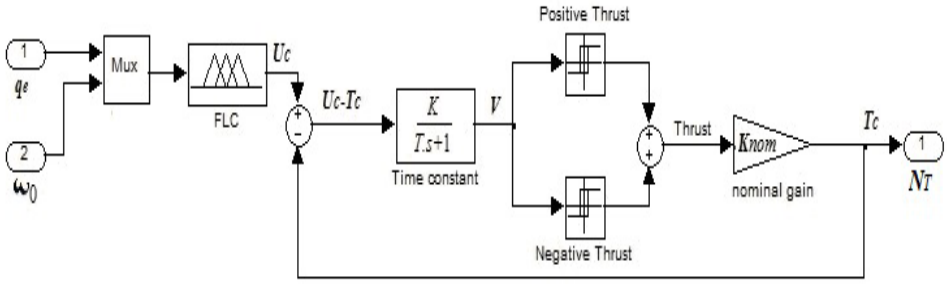

Fig. 2 – Fuzzy pulse width pulse frequency controller diagram.

The time behaviour of the output (V) of the time-constant network can be written in terms of its input ($U_c - T_c$) as,

$$\dot{V}\tau + V = K\ (U_c - T_c)\ , \tag{9}$$

where: U_c – output of FLC; T_c – oorque output; K – time constant network gain.

Performing Laplace transform for a constant step command we get,

$$V(s) = \frac{\tau V(0)}{1+\tau s} + \frac{K\ (U_c - T_c)}{s(1+\tau s)}\ . \tag{10}$$

The time domain solution of equation (10) is given as,

$$V(t) = V(0)\mathrm{e}^{-t/\tau} + K\,(U_c - T_c)[1 - \mathrm{e}^{-t/\tau}]\ . \tag{11}$$

Levels at which the trigger switches on and off are V_{on} and V_{off} respectively and the on and off pulse periods are denoted as t_{on} and t_{off} . Hence equation (11) can be re-written as,

$$V_{off} = V_{on}\mathrm{e}^{-t_{on}/\tau} + K\ (U_c - T_c)[1 - \mathrm{e}^{-t_{on}/\tau}]\ . \tag{12}$$

For a small value of t_{on}

$$t_{on} \approx \tau \frac{V_{on} - V_{off}}{V_{on} - K\ U_c + K\ T_c}\ . \tag{13}$$

Since the trigger is off, $T_c = 0$ which gives $(K\,(U_c - T_c) = KU_c)$. The trigger is then switched on at $V(t) = V_{on}$. Substitution of these terms into equation (11) becomes,

$$V_{on} = V_{off}\,\mathrm{e}^{-t_{off}/\tau} + K\ U_c[1 - \mathrm{e}^{-t_{off}/\tau}]\ . \tag{14}$$

Finally for a small value of t_{off}

$$t_{off} \approx \tau \frac{\boldsymbol{V}_{on} - \boldsymbol{V}_{off}}{\boldsymbol{K}\ \boldsymbol{U}_c + \boldsymbol{V}_{off}}. \tag{15}$$

Analysis of equations (13) and (15) shows that the pulse periods will be longer when $\boldsymbol{U}_c$ is large and this happens as soon as the reference input is applied. Also the frequency of pulse firings will be higher. As the error decreases and the attitude reaches the reference value the pulse periods become constant and the pulse frequency also decreases.

4. **SIMULATION RESULT**

The results presented in this section were obtained with a simulator that implements the dynamics of the satellite using C code, MATLAB and SIMULINK. A 98° inclination, circular orbit at an altitude of 650 km was used during the simulation tests, We assume that the total nitrogen is 7 kg. the following moment of inertia matrix is assumed. $\boldsymbol{I}$: diag [33.35 34.04 32.09]^T [kg m^2]. The magnetic moment in the orthogonal $\boldsymbol{X}$, $\boldsymbol{Y}$ and $\boldsymbol{Z}$-axes was assumed to be equal to 10 A m^2 each. An IGRF model was used to obtain the geomagnetic field values.

The satellite is left for two orbits starting from an initial attitude of 0° roll, 0° pitch, 0° yaw, 0 degree/second roll rate, $-2 \times \pi/6\,000$ degree/second pitch rate and 0 degree/second yaw rate. The Fig. 3 illustrate the progress of the satellite attitude, the thursters are enabled at 1200 second and a simultaneous –30° roll, 20° pitch and 45° yaw slew manoeuvre is commanded and next individually commanded back in reversed order. We compute the Euler angles root mean square error (RMSE) for the last orbit. It can be seen from Table 2 that the magnitude of the RMSE indicates there is no great difference between the controllers used.

Figs. 4, 5 and 6 shows the accumulated on-time of 25.51, 23.9 and 22.89 seconds for using PDBBC, PDPWPFC and FPWPFC respectively. This gives a total nitrogen fuel usage 3.419, 3.203 and 3.067 gram respectively. It can be noticed that the time required for the FPDWFC to drive the satellite to desired the state is shorter than that for the case of the PDBBC and PDPWPF.

The static simulations consist of 1000 Monte-Carlo runs by which the objective is to analyse the accuracy performance of the controllers system on low earth orbit satellite for 3axis thruster attitude control. For each Monte-Carlo run, an quaternions and angle rates was picked randomly from a population that spanned the 2-1-3 quaternion space; the starting attitude came from a uniform population between ± 45°. The Euler angle rates came from a uniform population between ± 0.01°/s. Deviation from nominal is 0.1 kgm^2 for the diagonal and off-diagonal terms of the spacecraft inertia tensor. The histogram of fuel consumption for all 1000 Monte-Carlo runs are shown in Fig. 7.

Table 2

RMSE attitude during 3-axis manoeuvres

	RMSE using PDBBC	RMSE using PDPWPF	RMSE using FPWPF
Roll (°)	0.34	0.42	0.48
Pitch (°)	0.62	0.62	0.52
Yaw (°)	0.43	0.42	0.48
Roll rate (°/s)	0.0030	0.0021	0.0023
Pitch rate (°/s)	0.0615	0.0619	0.0618
Yaw rate (°/s)	0.0019	0.0015	0.0017
	Magnitude of error	Magnitude of error	Magnitude of error
Angles (°)	0.83	0.86	0.85
Rate (°/s)	0.0617	0.0620	0.0619

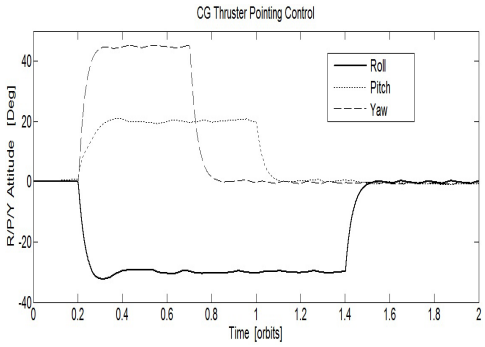

Fig. 3 – Attitude manoeuvres using 3-axis cold gas thruster control.

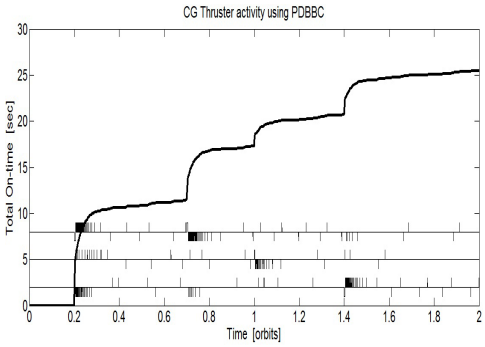

Fig. 4 – Cold gas thruster activity during 3-axis attitude manoeuvres using PDBBC.

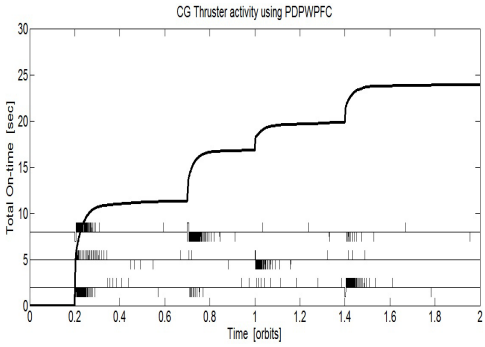

Fig. 5 – Cold gas thruster activity during 3-axis attitude manoeuvres using PDPWPFC.

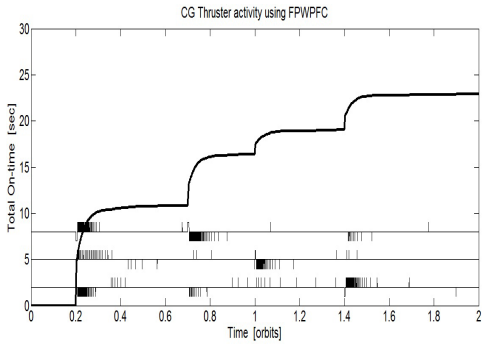

Fig. 6 – Cold gas thruster activity during 3-axis attitude manoeuvres using FPWPFC.

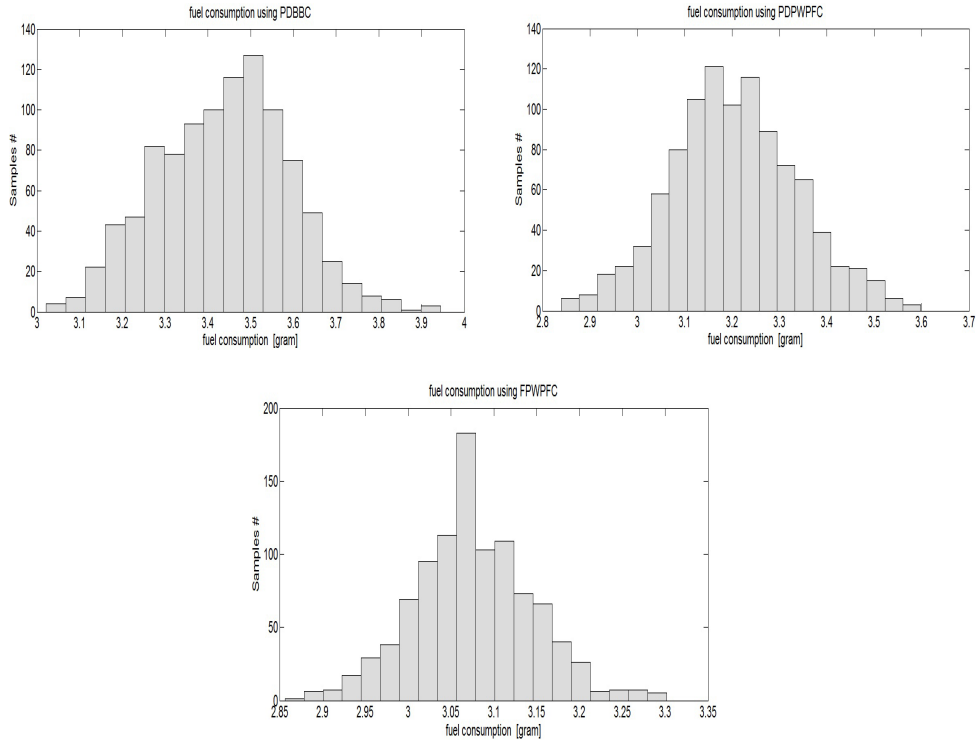

Fig. 7 – Histogram of fuel consumption for 1,000 Monte-Carlo runs
(number of occurrence $N1 + N2 + \cdots + N20 = 1{,}000$).

5. **CONCLUSION**

In this paper we proposed a thruster control technique based on the FPWPFC for a LEO micro-satellite. The simulation results show the important role that fuzzy logic plays in reducing and minimizing the fuel consumption. The simulation results indicate that the total On-time of the thruster activity required to drive the system to the desired state when using the FPWPFC is less than that PDBBC and PDPWPFC. The static simulations indicate that for 1000 runs the total nitrogen fuel usage about 2962 gram (42.31%) using the FPWPFC, 3248 gram (46.4%) and 3572 gram (51.02%) using PDPWPFC and PDBBC, respectively. The simulation results confirm dynamic control capabilities of these controllers under adverse conditions with regard to the variation of the most critical parameters and show that the FPWPFC has a minimum fuel consumption compared to PDPWPFC and PDBBC. This minimization can be improved by the optimization algorithms.

Received on November 20, 2012

REFERENCES

1. A. Bellar, M.K. Fellah, A.M. SI Mohammed, *Robust Attitude Control Using Fuzzy Sliding Mode for LEO Micro-satellite*, International Review of Automatic Control (IREACO), **5**, *2*, pp. 247-254, 2012.
2. I. Zuliana, Varatharajoo, Renuganth, *A study of reaction wheel configurations for a 3-axis satellite attitude control*, Advances in Space Research, **45**, *6*, pp. 750-759, 2010.
3. I. Hiroshi, N. Keiken, *A New Approach to Magnetic Angular Momentum Management for Large Scientific Satellites*, NEC Research & Development, **37**, *1*, pp. 60-77, 1996.
4. S. Thongchet, S. Kuntanapreeda, *Minimumtime Control of Satellite Attitude using a Fuzzy Logic Controller*, WSES International Conference on Fuzzy Sets & Fuzzy Systems (FSFS'01), Puerto De La Cruz, Spain, Februry 11-15, 2001.
5. G. Song, B.N. Agrawal, *Vibration reduction for flexible spacecraft attitude control using PWPF modulator and smart structures*, American Control Conference, **2**, pp. 161-172, 1999.
6. T.D. Krøvel, *PWPF modulation of thrusters on the micro-satellite SSETI/ESMO*, Technical report, Norwegian University of Science and Technology, Trondheim, Norway, 2004.
7. B. Wie, *Space Vehicle Dynamics and Control*, AIAA Education Series. Reston:American Institute of Aeronautics and Astronautics, Inc, 1998.
8. W. Song, Y. Liu, Q. Hu, *Spacecraft Vibration Suppression During Attitude Maneuver Using PWPF Modulated Input Component Commands*, Proceedings of the IEEE International Conference on Mechatronics & Automation Niagara Falls, 2005, Canada, pp. 493-498.
9. Q. Hu, Q, G. Ma, *Variable structure control and active vibration suppression of flexible spacecraft durung attitude maneuver*, published in Aerospace Science and Technology, 2005.
10. Q. Hu, *Robust integral variable structure controller and pulse-width pulse-frequency modulated input shaper design for flexible spacecraft with mismatched uncertainty/disturbance*, ISA Transactions, **46**, pp. 505-518, 2007.
11. Q. Hu, *Variable structure maneuvering control with time-varying sliding surface and active vibration damping of flexible spacecraft with input saturation*, Acta Astronautica, **64**, pp. 1085–1108, 2009.
12. R.Y. Chiang, Jyh-Shing Jang, *Fuzzy Logic Attitude Control for Cassini Spacecraft*, IEEE World Congress on Computational Intelligence, Orlando, FL, 1994.
13. N. Farrukh, S.K. Ahmed, A.A. Zainul Abidin, F.H Nordin, *Fuzzy bang–bang relay controller for satellite attitude control system*, Fuzzy Sets Syst, **161**, *15*, pp. 2104–2125, 2010.
14. A. Marwan, N. Farrukh, K.S.M Sahari, S. Hanim, *Robust Fuzzy MIMO Bang-Bang Controller for two Links Robot Manipulators*, Australian Journal of Basic and Applied Sciences, **5**, *12*, pp. 2071-2083, 2011.
15. N. Farrukh, A. Aidil, A. Talip, J. Nagi, A. Marwan, *Tuning of a New Fuzzy Bang-bang Relay Controller for Attitude Control System*, International Journal of Automation and Control, **5**, *2*, pp. 97-118, 2011.
16. B. Bouchiba, A. Hazzab, H. Gloui, M.K. Fellah, I.K. Bousserhane, P. Sicard, *Multiple-input Multiple-output Fuzzy Sliding Mode controller For Multi-Motors System*, Rev. Roum. Sci. Techn. – Électrotechn. et Énerg., **57**, *2*, pp. 202–211, 2012.
17. A. Kerboua, M. Abid, Hybrid Fuzzy Slding Mode Control of a Doubly-Fed Induction Generator in Wind Turbines, Rev. Roum. Sci. Techn. – Électrotechn. et Énerg., **57**, *4*, pp. 412–421, 2012.
18. J. R. Wertz, *Space mission analysis and design*, Space Technology Library, Kluwer Academic Publishers, Dordrecht, Boston, London, 1991.